Enumerative Combinatorics and Applications
ecajournal.haifa.ac.il
ECA **3:1** (2023) Article #S2R1
https://doi.org/10.54550/ECA2023V3S1R1

Combinatorics of Triangular Partitions

François Bergeron[†] and Mikhail Mazin[‡]

[†] *Department of Mathematics, Université du Québec à Montréal*
Email: bergeron.francois@uqam.ca

[‡] *Department of Mathematics, Kansas State University*
Email: mmazin@math.ksu.edu

Received: April 11, 2022, **Accepted**: September 1, 2022, **Published**: September 9, 2022

Abstract: The aim of this paper is to develop the combinatorics of constructions associated with what we call *triangular partitions*. As introduced in [9], these are the partitions whose cells are those lying below the line joining points $(r, 0)$ and $(0, s)$, for any given positive reals r and s. Classical notions such as Dyck paths and parking functions are naturally generalized by considering the set of partitions included in a given triangular partition. One of our striking results is that the restriction of the Young lattice to triangular partition has a planar Hasse diagram, with many nice properties. It follows that we may generalize the "first-return" recurrence, for the enumeration of classical Dyck paths, to the enumeration of all partitions contained in a fixed triangular one.

Keywords: Catalan Combinatorics; Triangular Partitions; Symmetric Functions
2020 Mathematics Subject Classification: 05A17; 05E10; 05E05

1. Introduction

The last 30 years have seen increasing and interesting interactions between the combinatorics of generalized Dyck paths and parking functions, Macdonald polynomials and operators, diagonal coinvariant spaces, Hilbert schemes of points, Khovanov-Rozansky homology of (m, n)-torus links, Double affine Hecke algebra, Elliptic Hall algebra, and Superspaces of bosons and fermions. The aim of this paper is to further the combinatorial study of the most general extension of the notion of Dyck paths that is involved in this context.

For the purpose of describing our overall setup, it is handy to consider classical Dyck paths as partitions $\alpha \subseteq \tau_{(n+1,n)}$ contained in the staircase partition $\tau_{(n+1,n)} := (n-1, n-2, \dots, 1, 0)$. These are well known to be enumerated by the Catalan numbers. From this point of view, parking functions are simply standard tableaux of skew shape $(\alpha + 1^n)/\alpha$, for any such α. Recall that the number $(n+1)^{n-1}$ in total. The generalization we consider here is obtained by changing the overall partition $\tau_{(n+1,n)}$ to other suitably chosen partitions τ. For instance, one may consider the more general staircase $\tau_{(jn+1,n)} := (j(n-1), j(n-2), \dots, k)$, for some $j \geq 1$. In that case, it is well known that the number of partitions included in $\tau_{(jn+1,n)}$ is given by the Fuss-Catalan number $1/(jn+1)\binom{(j+1)n}{n}$. The corresponding number of parking functions is given by the simple formula $(jn+1)^{n-1}$. In the historical sequence of generalizations, *Rational Catalan Combinatorics* (see [1]) comes next in line, with an overall partition consisting of the set of cells lying below the diagonal of a $(k \times n)$-rectangle, with k and n coprime. The terminology "rational" alludes to k/n being a rational number. Removing the coprimality condition, one gets *Rectangular Catalan Combinatorics* (see [5]).

The final step in the hierarchy, introduced in [9], corresponds to choosing any overall "triangular partition". These are the partitions whose cells are those lying below the line joining points $(r, 0)$ and $(0, s)$, for any given positive reals r and s. The resulting partitions*, are here denoted by τ_{rs}. As mentioned previously, the rational case corresponds to choosing $r = k$ and $s = n$, relatively prime integers, and it is well known that the number of partitions contained in τ_{kn} is given by the formula $\frac{1}{k+n}\binom{k+n}{n}$, whilst the number of associated parking functions is k^{n-1}. These enumerations become a bit trickier when one drops the coprimality requirement[†], taking the

*These are defined in section 2.
[†]This is the "rectangular" case.

respective forms

$$\sum_{\mu\vdash d} \frac{1}{z_\mu} \prod_{j\in\mu} \frac{1}{a+b}\binom{j(a+b)}{jb}, \qquad \text{and} \qquad \sum_{\mu\vdash d} \frac{n!}{z_\mu} \prod_{j\in\mu} \frac{(ja)^{jb}}{a\,(jb)!},$$

where $a := k/d$, $b := n/d$, for $d = \gcd(k,n)$; and writing $j \in \mu$ for j being a part of μ. Recall here that $z_\mu := \prod_i i^{d_i}\, d_i!$, with d_i being the number of i-size parts of μ.

The extension to any triangular partitions, when r and s are any positive real numbers, is motivated by the results in [9]. The purpose of this paper is to explore different aspects of this most general framework. We start with a discussion of the properties and intrinsic characterization of triangular partitions, including interesting aspects of the dominance and containment order. We then obtain general recurrence for the (weighted) enumeration of triangular Dyck paths and associated parking functions (see Proposition 6.1 and Proposition 8.1).

2. Triangular partitions

A partition $\tau = \tau_1\tau_2\cdots\tau_k$ is said to be **triangular** if there exist positive real numbers r and s such that

$$\tau_j = \lfloor r - j\,r/s \rfloor,$$

with j running over integers that are less or equal to s. In other words, the cells $c = (i,j) \in \mathbb{N}^2$ of the triangular partition τ_{rs} are those that lie below the line joining $(0,s)$ to $(r,0)$, *i.e.*

$$(i,j) \in \tau_{r,s} \qquad \text{iff} \qquad \frac{i+1}{r} + \frac{j+1}{s} \le 1.$$

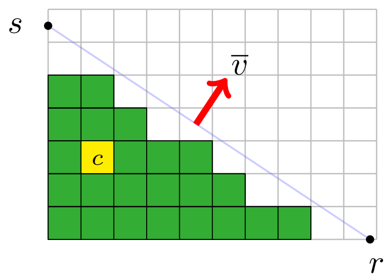

Figure 1: Triangular partition.

We say that this line **cuts off** τ. Clearly, the conjugate of a triangular partition is triangular. Triangular partitions have been considered under the name "plane corner cuts" in [15] and enumerated in [10]. Denoting by t_N the number of triangular partitions of size N, small values of the sequence $\{t_N\}_N$ are:

$$1, 1, 2, 3, 4, 6, 7, 8, 10, 12, 13, 16, 16, 18, 20, 23, \ldots$$

Figure 2 displays all triangular partitions of $N \le 6$, with ε denoting the "empty" partition.

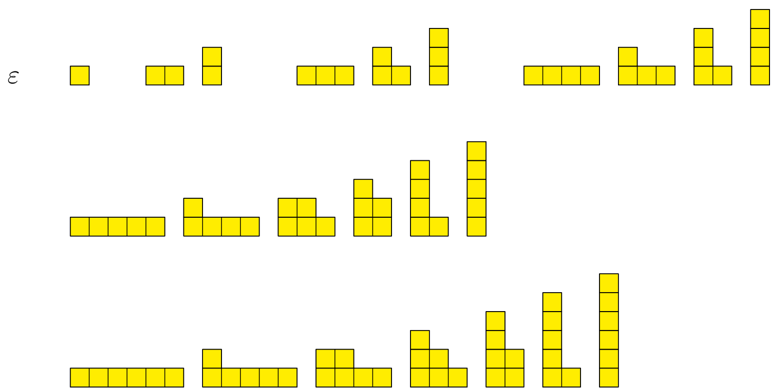

Figure 2: All triangular partitions, for $n \le 6$.

Observe that many different pairs (r,s) may give rise to the same triangular partition τ. Indeed, as illustrated in Figure 4, we have $\tau = \tau_{rs} = \tau_{r's'}$ whenever there are no positive integer coordinate points lying between the lines $x/r + y/s = 1$ and $x/r' + y/s' = 1$. In particular, $\tau_{rn} = \tau_{kn,n}$ for all $kn \le r \le kn+1$ and $k, n \in \mathbb{N}$.

We say that the line $x/r + y/s = 1$ **touches** the cell (i,j) (from above) if it contains the north-east corner of the cell, *i.e.* $(i+1)/r + (j+1)/s = 1$. If the line $x/r + y/s = 1$ touches no cells, then $\tau_{r's'} = \tau_{rs}$ for any (r',s') close enough to (r,s). If the line $x/r + y/s = 1$ touches a cell (i,j), then taking $r' = r - \epsilon$ and $s' = s - \epsilon$, for a sufficiently small positive ϵ, one may "remove" the cell (i,j) from the diagram of the partition. On the other hand, taking $r' = r + \epsilon$ and $s' = s + \epsilon$ we get a line cutting off the same partition while touching no cells. Summing up, for every triangular partition τ there is a pair (r,s) such that the line $x/r + y/s = 1$ cuts off τ, without touching any cell.

Let us say that τ is **integral**, if there exist k and n in $\mathbb{N}$ such $\tau = \tau_{kn}$. As mentioned previously, these are the triangular partitions that give rise to the previous context of "rectangular" Catalan combinatorics; and adding the requirement that $\gcd(k,n)=1$ that of "rational" Catalan combinatorics. Clearly, conjugation preserves integrality. For size $N \le 10$, the non-integral triangular partitions are the following:

$$\begin{aligned}\{&2111, 221, 32, 41,\\ &21111, 51,\\ &211111, 3211, 421, 61,\\ &2111111, 221111, 22211, 53, 62, 71,\\ &21111111, 2211111, 3321, 432, 72, 81,\\ &211111111, 22111111, 322111, 33211, 532, 631, 82, 91\}.\end{aligned}$$

As N grows, non-integral triangular partitions become preponderant. For instance, among all triangular partitions of size at most 55, more than 87.5% of them are non-integral. Thus triangular partitions significantly extend the field of study.

A **slope vector** for a triangular partition τ is a positive coordinate vector that is orthogonal to one of the lines that cut off τ. If need be, we may normalize slope vectors so that their coordinates sum up to 1. For any two lines cutting off the same triangular partition τ, say with respective slope vectors $(t_1, 1-t_1)$ and $(t_2, 1-t_2)$, there exists a line with slope vector $(t, 1-t)$ that also cuts of τ for any $t_1 < t < t_2$. By definition, a triangular partition affords (infinitely many) slope vectors. Hence, it follows that:

Lemma 2.1. *The closure of the set of all slope vectors of a triangular partition τ forms a convex cone C_τ, of the form*

$$C_\tau = \{\lambda(t, 1-t) \,|\, t_\tau^- \le t \le t_\tau^+,\ \lambda \in \mathbb{R}_+\}, \tag{1}$$

for some $0 \le t_\tau^- < t_\tau^+ \le 1$. Moreover, τ is uniquely characterized by its size and the pair (t_τ^-, t_τ^+).

We will further discuss this unicity below, but first, we show how to explicitly calculate t_τ^- and t_τ^+. As we will see, this also gives a direct characterization of triangular partitions, without having to exhibit a cutting line.

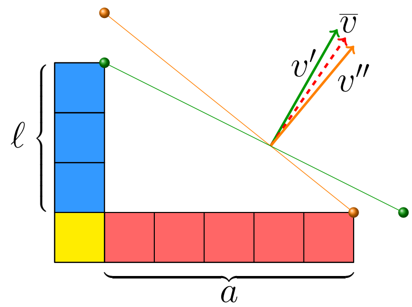

Figure 3: The two extreme slope vectors (here upscaled) of a hook shape $(a \,|\, \ell)$.

For a cell c of a partition μ, recall that the **hook** of c is the partition of shape $(a+1, 1^\ell)$, with $a = a_\mu(c)$ and $\ell = \ell_\mu(c)$ standing for the **arm** and **leg** of $c = (i,j)$ of μ. Recall that $a_\mu(c) := \mu_j - i$ (resp. $\ell_\mu(c) := \mu'_i - j$) is the number of cells of μ that sit to the right of (resp. above) c in the same row (resp. column). The **hook length** of cell c in μ, is defined to be $\varepsilon(c) = \varepsilon_\mu(c) := 1 + a_\mu(c) + \ell_\mu(c)$. The "Frobenius notation" for such a hook is $(a \,|\, \ell)$.

For any given cell c of a partition μ, we consider the vectors $(t'(c), 1-t'(c))$ and $(t''(c), 1-t''(c))$ respectively orthogonal to the lines:

- which joins the vertices $(1, \ell(c)+1)$ and $(a(c)+2, 1)$, and
- which joins the vertices $(1, \ell(c)+2)$ and $(a(c)+1, 1)$.

An instance is illustrated in Figure 3. It is easy to check that

$$t'_\mu(c) := \ell(c)/\varepsilon(c), \qquad \text{and} \qquad t''_\mu(c) = (\ell(c)+1)/\varepsilon(c). \tag{2}$$

When τ is a triangular partition, all of its slope vectors $v = (t, 1-t)$ must be such that $t'_\tau(c) < t < t''_\tau(c)$. Indeed, all the cells appearing in the hook of c must lie below (up to parallel shift) any line that cuts off τ, with $t'_\tau(c)$ and $t''_\tau(c)$ giving extreme bounds. Otherwise, an extra cell would have to lie in τ, either at the end of the arm or the leg of c.

Vice versa, if the condition $t'_\tau(c) < t < t''_\tau(c)$ is satisfied for every cell c in τ, then $(t, 1-t)$ is a slope vector of τ. Indeed, consider the lowest line (r, s) perpendicular to $(t, 1-t)$ and such that $\tau \subset \tau_{rs}$. It follows that the line (r, s) touches a cell of c' of τ. Suppose that there is a cell c'' that fits under the line (r, s), but such that $c'' \notin \tau$. Without loss of generality, we can assume that c' lies to the west of c''. Let $c \in \tau$ be the cell in the same column as c' and the same row as c''. Then $t \geq t''_\tau(c)$ which is a contradiction. Hence there is no such cell c'' and $\tau = \tau_{rs}$ We have thus shown the following:

Lemma 2.2. *A partition τ is triangular if and only if $t^-_\tau < t^+_\tau$, with*

$$t^-_\tau := \max_{c \in \tau} \frac{\ell(c)}{a(c) + \ell(c) + 1}, \qquad \text{and} \qquad t^+_\tau := \min_{c \in \tau} \frac{\ell(c) + 1}{a(c) + \ell(c) + 1}. \tag{3}$$

Furthermore, if $t^-_\tau < t^+_\tau$ then $(t, 1-t)$ is a slope vector of τ if and only if $t^-_\tau < t < t^+_\tau$.

As illustrated in Figure 4, this gives an explicit description for the extreme rays of the cone C_τ which does not rely on explicit knowledge of a line cutting off τ. Setting $t_\tau := (t^-_\tau + t^+_\tau)/2$, we may consider the vector $v_\tau := (t_\tau, 1 - t_\tau)$ to be a "standard" **slope vector** for τ.

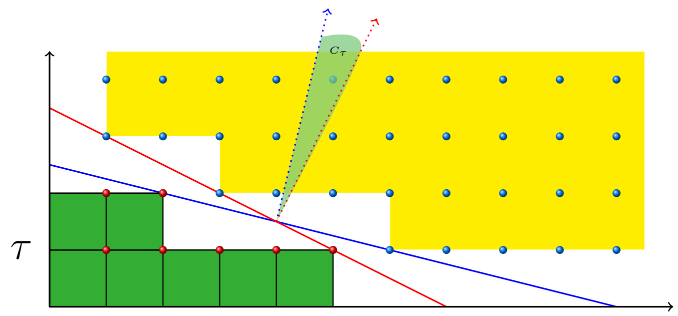

Figure 4: The cone of a triangular partition.

Two triangular partitions are said to be **similar**‡ if they share a slope vector. For any triangular partition τ, it is easy to check that all partitions associated to τ-**shadows** of a cell $c = (i, j)$:

$$\mathrm{sh}_c(\tau) := \{(x, y) \,|\, (x, y) \in \tau, \ \text{with } x \geq i \text{ and } y \geq j\},$$

are similar to τ. For any fixed $t \geq 0$, all the partitions with cell sets:

$$\{(i, j) \,|\, i\, t + j\, (1 - t) < d\}, \qquad 0 \leq d < \infty,$$

are clearly similar, since they share the slope vector $(t, 1-t)$. These partitions are nested as d grows. Furthermore, if one chooses t so that $t/(1-t)$ is irrational, cells are added one at a time as d grows. We get the following

Corollary 2.1. *For a fixed size n, there are finitely many values*

$$0 = t_0 < t_1 < \ldots < t_k < 1 = t_{k+1}$$

such that for every $i \in \{0, 1, \ldots, k+1\}$ no triangular partition of size n admits a slope vector $(t_i, 1 - t_i)$. Furthermore, for every $i \in \{0, 1, \ldots, k\}$ there is a unique triangular partition τ_i of size n such that $t^-_{\tau_i} = t_i$ and $t^+_{\tau_i} = t_{i+1}$.

Note

Part of the study of triangular partitions may be coined in terms of "sturmian" words. Indeed, these give explicit descriptions of discrete lines in the plane. Their factors, also known as "mechanical" words, describe segments of discrete lines. The upper bound (cells closest to a cutting line) of triangular partitions correspond to such a segment. However, this approach does not emphasize the number of cells lying below the line. For more on sturmian and mechanical words, see [13, Chapter 2].

‡Careful, this is not intended to be an equivalence relation.

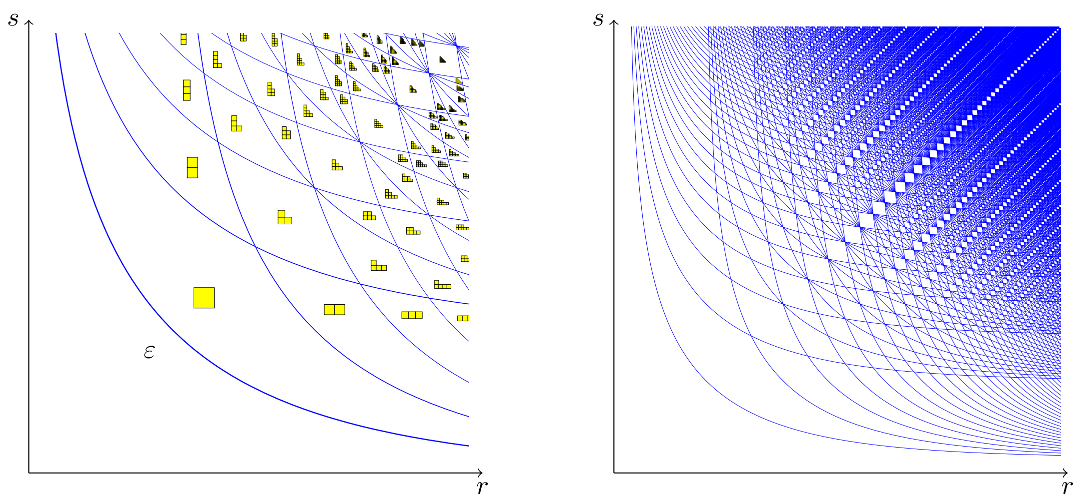

(a) With regions labeled

(b) Larger portion

Figure 5: Triangular partition regions, in logarithmic scale.

3. Moduli space of lines

Note that a line $x/r + y/s = 1$ touches a cell $(i, j) = (a-1, b-1)$ if and only if

$$a/r + b/s = 1 \quad \text{iff} \quad as + br = rs \quad \text{iff} \quad (r-a)(s-b) = ab.$$

Therefore the positive (r, s)-quadrant $\mathcal{Q} := (\mathbb{R}_{>0})^2$ is can be decomposed into regions by (positive branches of) hyperbolas with equations as above, one for each cell. Thus $\mathcal{Q}$ may be considered as a **moduli space of lines**. In this moduli space, the hyperbola

$$\mathcal{H}_{ab} := \{(r, s) \in \mathcal{Q} \,|\, (r-a)(s-b) = ab\},$$

associated to a cell $(i, j) = (a-1, b-1)$, separates $\mathcal{Q}$ according to whether the cell (i, j) fits below the line (r, s), is touched by the line (r, s), or does not fit under it. These possibilities respectively correspond to

$$(r-a)(s-b) > ab, \qquad (r-a)(s-b) = ab, \qquad \text{and,} \qquad (r-a)(s-b) < ab.$$

Thus the cells occurring in a triangular partition specified by (r, s) are in bijection with the hyperbolas separating (r, s) from the origin. In other words, as one crosses the hyperbola $\mathcal{H}_{ab}$, going towards the origin, the cell $(i, j) = (a-1, b-1)$ gets removed from the partition. For this reason it is natural to say that $\mathcal{H}_{ab}$ is the **hyperbolic wall** associated to (a, b).

Lemma 3.1. *There is a bijective natural map*[§] $\rho : \mathcal{C} \to \mathcal{T}$, *from the set* $\mathcal{C}$ *of connected components of the complement:*

$$\overline{\mathcal{Q}} := \mathcal{Q} \setminus \bigcup_{(a,b)\in\mathbb{N}^2} \mathcal{H}_{ab},$$

to the set $\mathcal{T}$ *of triangular partitions.*

Proof. Consider the map that sends the (r, s)-line in $\overline{\mathcal{Q}}$ to the partition τ_{rs}. As observed above, this is a locally constant map from $\overline{\mathcal{Q}}$ to the set of triangular partitions. Therefore, it is well defined on connected components. The surjectivity is immediate, since by definition a triangular partition τ is cut off by some line $x/r + y/s = 1$, and we have observed that (r, s) may be chosen so that this line contains no points of $\mathbb{N}^2$. To prove injectivity one needs to show that whenever two points of $\overline{\mathcal{Q}}$ define the same triangular partition, then they must lie in the same connected component. We consider two cases.

First, when the lines associated to (r_0, s_0) and (r_1, s_1) do not intersect in the positive quadrant, then one may assume without loss of generality that $r_0 \le r_1$ and $s_0 \le s_1$. Let us show that the segment $(r_t, s_t) := (r_0 + t(r_1 - r_0), s_0 + t(s_1 - s_0))$, connecting these two points of $\mathcal{Q}$, lies entirely within the same connected component of $\overline{\mathcal{Q}}$. Indeed, if the segment $(r_t, s_t)_{0\le t\le 1}$ would cross one of the hyperbolic walls $\mathcal{H}_{ab}$, then there would exist some $0 < t < 1$ such that the line $x/r_t + y/s_t = 1$ passes through (a, b). The partition corresponding

[§]Illustrated in Figure 5.

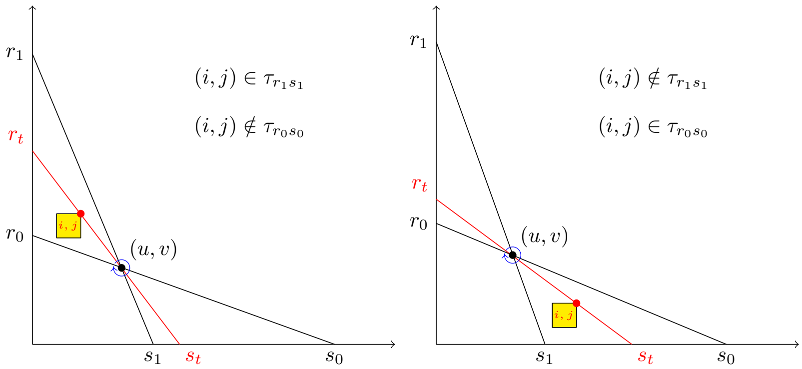

Figure 6: Illustration of Lemma 3.1.

to (r_1, s_1) would thus contain the cell $(i,j) = (a-1, b-1)$, whereas the partition corresponding to (r_0, s_0) would not; which is a contradiction.

If the lines associated to (r_0, s_0) and (r_1, s_1) intersect in the positive quadrant (as illustrated in Figure 6), say at some (non-integer) point (u,v), then both points (r_0, s_0) and (r_1, s_1) belong to the hyperbola $(r-u)(s-v) = uv$. As one moves along this hyperbola, associated lines rotate around (u,v). Without loss of generality, one may assume that $r_0 \le r_1$ and $s_0 \ge s_1$. Consider the segment of the hyperbola $(r-u)(s-v) = uv$ lying between the points (r_0, s_0) and (r_1, s_1). Suppose that for some point (r_t, s_t) on this segment the line $x/r_t + y/s_t = 1$ passes through an integer point (a,b). If $a < u$, then it follows that the triangular partition corresponding to (r_1, s_1) contains the cell $(i,j) = (a-1, b-1)$, whereas the partition corresponding to (r_0, s_0) does not. Similarly, if $a > u$, then the triangular partition corresponding to (r_0, s_0) contains the cell $(i,j) = (a-1, b-1)$, whereas the partition corresponding to (r_1, s_1) does not. Moreover, $a \ne u$ since the hyperbola $(r-u)(s-v) = uv$ can only intersect a vertical line at one point. Therefore, we get a contradiction in this case as well. □

Let τ be a triangular partition, and set

$$\mathcal{R}_\tau := \mathrm{CL}\big\{(r,s) \in \mathcal{Q} \,\big|\, x/r + y/s = 1 \text{ cuts off } \tau\big\}.$$

This is the closure of the connected component corresponding to τ by the above lemma. Observe that, for any (r,s) in the interior $\mathcal{R}_\tau^\circ$, the line $x/r + y/s = 1$ does not touch any cells. With this terminology, the bijective map of Lemma 3.1 sends $\mathcal{R}_\tau^\circ \mapsto \tau$.

We say that a cell of a triangular partition τ is **removable** if it can be removed so that the resulting partition is also triangular. Similarly, we say that a cell of the complement of τ is **addable** if it can be added to τ so that the resulting partition is also triangular. An argument similar to the proof of Lemma 3.1 proves the following:

Lemma 3.2. *Let (i,j) be a removable cell of a triangular partition τ. Then there exists $(r,s) \in \mathcal{R}_\tau$ such that (i,j) is the unique cell touched by the line $x/r + y/s = 1$.*

Proof. Consider (r_0, s_0) such that the line $x/r_0 + y/s_0 = 1$ cuts off $\tau \setminus \{(i,j)\}$, and (r_1, s_1) such that the line $x/r_1 + y/s_1 = 1$ cuts off τ. If these lines do not intersect in the positive quadrant, then $r_0 < r_1$, $s_0 < s_1$, and $(a,b) = (i+1, j+1)$ is the only integer point that lies between the lines. Then for some $0 < t < 1$, with $r_t = r_0 + t(r_1 - r_0)$ and $s_t = s_0 + t(s_1 - s_0)$, the line $x/r_t + y/s_t = 1$ cuts off τ and touches the cell (i,j), while not touching any other cells.

Suppose the lines $x/r_0 + y/s_0 = 1$ and $x/r_1 + y/s_1 = 1$ intersect at some positive point (u,v). One can choose these lines so that they do not pass through integer points, ensuring that (u,v) is not integral. Let us assume that $a = i+1 < u$ (the case $a > u$ is obtained similarly). The triangle bounded by the lines and the vertical axis contains the unique integer point $(a,b) = (i+1, j+1)$, while the triangle bounded by the lines and the horizontal axis does not contain integer points. Therefore, the line connecting (a,b) and (u,v) cuts off τ and touches the unique cell (i,j). □

The following Lemma can be observed directly, but it is especially natural from the point of view of the moduli space of lines $\mathcal{Q}$:

Lemma 3.3. *Consider a line $x/r + y/s = 1$. Let $(i_1, j_1), (i_2, j_2), \ldots, (i_k, j_k)$ be all the cells touched by $x/r + y/s = 1$, ordered so that $i_1 < i_2 < \ldots < i_k$. Then the set of triangular partitions β such that $(r,s) \in \mathcal{R}_\beta$ is the union of the following:*

1. τ_{rs},

2. $\beta := \tau_{rs} - \{(i_1, j_1), (i_2, j_2), \dots, (i_k, j_k)\}$,

3. $\{\tau_{rs} - \{(i_l, j_l), (i_{l+1}, j_{l+1}), \dots, (i_k, j_k)\} \,|\, 1 < l \leq k\}$,

4. $\{\tau_{rs} - \{(i_1, j_1), (i_2, j_2), \dots, (i_l, j_l)\} \,|\, 1 \leq l < k\}$.

Indeed, there are k hyperbolas intersecting at (r, s), and these partitions correspond to the $2k$ connected components of $\overline{\mathcal{Q}}$ near (r, s). Note that only two of the cells $(i_1, j_1), \dots, (i_k, j_k)$ in τ_{rs} are removable: (i_1, j_1) and (i_k, j_k). In cases (3) and (4) of the Lemma the only removable cell touched by the line $x/r + y/s = 1$ is (i_l, j_l). Similarly, of the cells $(i_1, j_1), \dots, (i_k, j_k)$ only (i_1, j_1) and (i_k, j_k) are addable for β, and in the cases (3) and (4) the only addable cells touched by the line $x/r + y/s = 1$ are (i_{l-1}, j_{l-1}) and (i_{l+1}, j_{l+1}) respectively.

4. Orders on triangular partitions

Two orders are of interest here, both obtained by restriction of classical orders on partitions to triangular partitions. First, even though the **dominance order** is only a partial order on all partitions of a given size¶, its restriction to triangular partitions is a total order which we denoted by $\alpha \preceq \beta$. See Figure 7 for an illustration of the difference between the two contexts. It is easy to show that

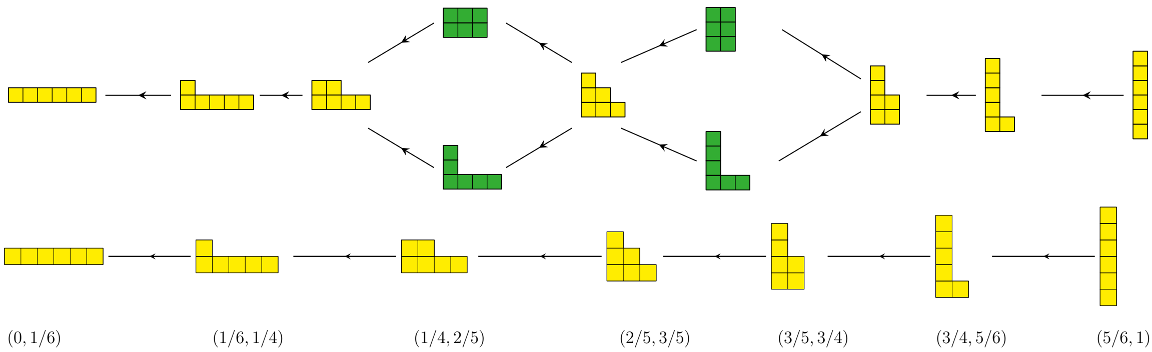

Figure 7: The dominance order on all partitions of 6, and its restriction to triangular ones.

Lemma 4.1. *For two same size triangular partitions α and β, we have $\alpha \prec \beta$ if and only if $t_\alpha^+ \leq t_\beta^-$. Furthermore, β covers α in dominance order if and only if $t_\alpha^+ = t_\beta^-$.*

Proof. According to Corollary 2.1, $(t, 1-t)$ is not a slope vector of any triangular partition of size n if and only if there exist triangular partitions α and β of size n, such that $t = t_\alpha^+ = t_\beta^-$. Let $x/r + y/s = 1$ be the closest to the origin line with the slope vector $(t, 1-t)$ such that $|\tau_{rs}| > n$. It follows then that $x/r + y/s = 1$ touches more than one cell. Similar to Lemma 3.3, let $(i_1, j_1), (i_2, j_2), \dots, (i_k, j_k)$ be all the cells touched by $x/r + y/s = 1$, ordered so that $i_1 < i_2 < \dots < i_k$. Let $l := |\tau_{rs}| - n$. One gets $l < k$ by the definition of the line $x/r + y/s = 1$. Partition $\tau_{rs} - \{(i_1, j_1), \dots, (i_l, j_l)\}$ is of size n and can be cut off by a line with a slope vector $(t - \epsilon, 1 - t + \epsilon)$ for a small enough $\epsilon > 0$. Indeed, one should rotate the line $x/r + y/s = 1$ counterclockwise around the north-east corner of the cell (i_{l+1}, j_{l+1}) a little. Therefore, $\alpha = \tau_{rs} - \{(i_1, j_1), \dots, (i_l, j_l)\}$. By a similar consideration, one can obtain that $\beta = \tau_{rs} - \{(i_{k-l+1}, j_{k-l+1}), \dots, (i_k, j_k)\}$. Finally, one observes that $\alpha \prec \beta$ and the rest of the Lemma follow from Corollary 2.1. □

In simple terms, if one lists the same size triangular partitions in clockwise order of their slope vectors, they will occur in decreasing dominance order. For size 6, this is illustrated in Figure 7. More properties of the dominance order on triangular partitions (with different terminology) may be found in [14].

Our second order of interest is the restriction of the containment order $\alpha \subseteq \beta$ to triangular partitions. This gives rise to the **Triangular Young poset**, which we denoted by $\mathbb{Y}_\triangle$. We denote the cover relation in $\mathbb{Y}_\triangle$ by $\alpha \lessdot \beta$.

Lemma 4.2. *Let α and β be triangular partitions and $\alpha \subset \beta$. Then one has $\alpha \lessdot \beta$ if and only if α is obtained from β by removing exactly one cell. In particular, $\mathbb{Y}_\triangle$ is ranked by the number of cells in a partition.*

Proof. Clearly, if α is obtained from β by removing exactly one cell, then $\alpha \lessdot \beta$. Suppose now that $\alpha \lessdot \beta$ and $|\beta| > |\alpha| + 1$. Let $\alpha = \tau_{r_0 s_0}$ and $\beta = \tau_{r_1 s_1}$. Similar to Lemma 3.1, let us connect the points (r_0, s_0) and

¶Starting with size 6.

(r_1, s_1) of the moduli space $\mathcal{Q}$ by a path (r_t, s_t) as follows: if the corresponding lines do not intersect inside the positive quadrant, then take the straight line $(r_t, s_t) = (r_0 + t(r_1 - r_0), s_0 + t(s_1 - s_0))$; if they intersect, then take their rotation around the point of intersection. Observe that in both cases the partition $\tau_{r_t s_t}$ can only increase as t increases. Indeed, even for the rotation, if a cell gets removed, it is not going to be added back later, which contradicts $\tau_{r_0 s_0} = \alpha \subset \beta = \tau_{r_1 s_1}$. Since $\alpha \lessdot \beta$ it follows that all cells from $\beta - \alpha$ have to be added simultaneously, at a certain value $0 < t < 1$, which means that the line $x/r_t + y/s_t = 1$ touches all the cells of $\beta - \alpha$. Then Lemma 3.3 guarantees that the cells can be added one by one. Hence we get a contradiction. □

Corollary 4.1. *Modulo the map $\rho : \mathcal{C} \to \mathcal{T}$ from Lemma 3.1, the cover relation of $\mathbb{Y}_\triangle$ corresponds to crossing a hyperbolic wall at a generic point.*

In other words, the Hasse diagram of $\mathbb{Y}_\triangle$ is planar: for every triangular partition, τ one can draw the vertex corresponding to it at the center of the region $\mathcal{R}_\tau$, and then connect vertices in the neighboring regions by crossing the shared pieces of the boundary at simple points. Note that the resulting drawing of the Hasse diagram satisfies an additional condition:

Lemma 4.3. *For any interval $[\alpha, \beta] \subset \mathbb{Y}_\triangle$, the vertices corresponding to α and β in the planar presentation of the Hasse diagram of $[\alpha, \beta]$ obtained by restricting the above construction to $[\alpha, \beta]$ both belong to the boundary of the unbounded region. In particular, the graph obtained from the Hasse diagram of $[\alpha, \beta]$ by adding an extra edge connecting α to β is planar.*

Proof. Indeed, the regions corresponding to the partitions not in the interval $[\alpha, \beta]$ are inside the unbounded region of the Hasse diagram of $[\alpha, \beta]$, and unless $\alpha = \emptyset$, both $\mathcal{R}_\alpha$ and $\mathcal{R}_\beta$ share boundaries with regions corresponding to partitions outside of $[\alpha, \beta]$. If $\alpha = \emptyset$ then the corresponding vertex is also clearly on the boundary of the unbounded region. □

Lemma 4.1 also implies that

Corollary 4.2. *In the Hasse diagram of Figure 8, triangular partitions of the same size appear from left to right in decreasing dominance order.*

There is a subtle difference between the planarity of the Hasse diagram as an abstract graph and its planarity as a Hasse diagram: in a Hasse diagram, the edges are required to be drawn going upward from the smaller element to the bigger element, with respect to a chosen direction. See [16] for a detailed discussion of the planarity of Hasse diagrams and its connection to the condition in Lemma 4.3.

Lemma 4.4. *The poset $\mathbb{Y}_\triangle$ is a lattice.*

Proof. Since $\mathbb{Y}_\triangle$ is bounded from below, it suffices to show that the join operation is well defined. Clearly, for any two triangular partitions α' and β' there exists a common upper bound, i.e. a triangular partition τ such that $\alpha' \subset \tau$ and $\beta' \subset \tau$. Therefore, we only need to prove that the minimal upper bound is unique.

Suppose that $A \neq B$ are two minimal upper bounds for α' and β'. Consider a saturated chain connecting α' to A, and let α be the maximal element on that chain such that $\alpha \subset B$. Similarly, consider a saturated chain connecting β' to B, and let β be the maximal element on that chain such that $\beta \subset A$. Consider also saturated chains connecting α to B and β to A. Note that all four chains connecting α and β to A and B cannot intersect each other except at the ends. In particular, they correspond to non-intersecting paths on the Hasse diagram.

Let τ be a minimal upper bound for A and B, let T be a maximal lower bound for α and β, and consider saturated chains connecting T to α and β, and A and B to τ. Note that the corresponding paths on the Hasse diagram do not intersect between each other or with the previously constructed four paths (except at the ends). Finally, Lemma 4.3 guarantees that if we restrict the drawing of the Hasse diagram to the interval $[T, \tau] \subset \mathbb{Y}_\triangle$, than the vertices corresponding to τ and T are going to be on the boundary of the unbounded region, and, therefore, can be connected by an extra path not intersecting any edges of the Hasse diagram of the interval $[T, \tau]$. Thus we obtained a planar presentation of a $K_{3,3}$ graph: every vertex of τ, α, β is connected to every vertex of T, A, B, and all the connecting paths do not intersect each other except at the ends. Contradiction. □

A lower portion of this Hasse diagram is illustrated in Figure 8. It is dual corresponds to Figure 5. For obvious reasons, nodes and regions are unlabeled in the larger right-hand side images. The larger image of the poset displays all triangular partitions of $n \leq 45$. Its vertices are equal to $n\, v_\tau$ (up to a logarithmic rescaling and $\pi/4$ rotation), with v_τ the standard[‖] slope vector of τ. The lattice $\mathbb{Y}_\triangle$ is not a distributive, as illustrated by the fact that we have $221 \vee (32 \wedge 211) \neq (221 \vee 32) \wedge (221 \vee 211)$.

Let us prove a few more results about the triangular Young poset $\mathbb{Y}_\triangle$ and the structure of the moduli space of lines $\mathcal{Q}$.

[‖] See definition after Lemma 2.2.

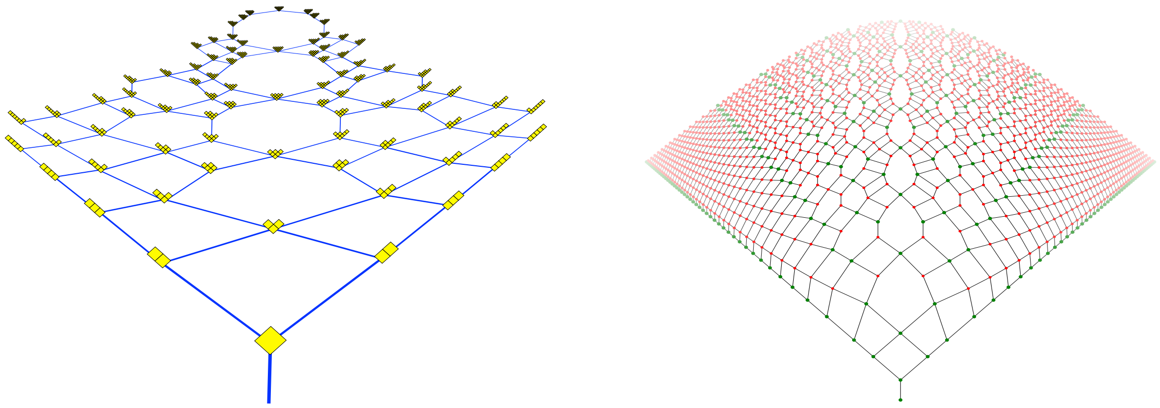

(a) With labeled nodes (b) Larger portion

Figure 8: Bottom of Triangular Young poset $\mathbb{Y}_\triangle$ (red vertices non-integral).

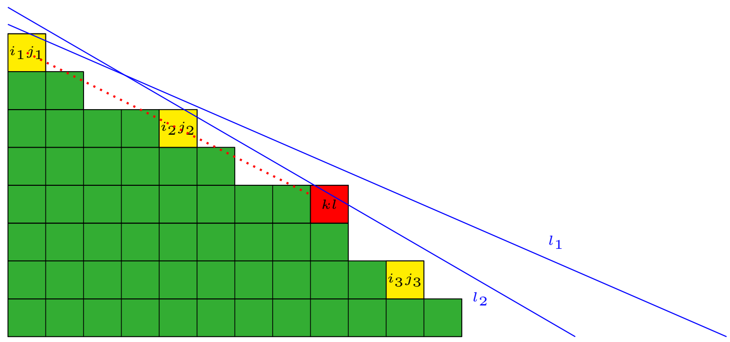

Figure 9: Illustration of Lemma 4.5.

Lemma 4.5. *No triangular partition can have more than* 2 *removable cells. Similarly, no triangular partition can have more than* 2 *addable cells.*

Proof. Suppose that a triangular partition α has three removable cells (i_1, j_1), (i_2, j_2), and (i_3, j_3), $i_1 < i_2 < i_3$. It follows that the cell (i_2, j_2) cannot fit under the line touching the cells (i_1, j_1) and (i_3, j_3). Otherwise, in order to remove the cell (i_2, j_2) one would either have to remove the cell (i_1, j_1) or (i_3, j_3).

Without loss of generality, one may assume that $i_2 - i_1 \leq i_3 - i_2$, which implies $j_1 - j_2 \leq j_2 - j_3$. There is then a cell

$$(k, l) := (i_2 + (i_2 - i_1), j_2 + (j_2 - j_1)),$$

since $j_2 + (j_2 - j_1) \geq j_2 + (j_3 - j_2) = j_3 \geq 0$ and $i_2 + (i_2 - i_1) > 0$. Consider the lines ℓ_1 and ℓ_2 respectively cutting off $\alpha - \{(i_1, j_1)\}$ and $\alpha - \{(i_2, j_2)\}$. The cell (k, l) fits under the line ℓ_1, but it does not fit under the line ℓ_2; hence we have a contradiction. The statement about addable cells is proved analogously. □

One case of Lemma 4.5 is illustrated in Figure 9. Here the line l_1 cuts off $\alpha - \{(i_1, j_1)\}$ and the line l_2 cuts off $\alpha - \{(i_2, j_2)\}$. Then the box (k, l) fits under l_1, but not under l_2.

Lemma 4.6. *Suppose that a triangular partition τ corresponds to an unbounded region. Then τ is either empty, a row partition, or a column partition.*

Proof. Indeed, if both cells $(1, 0)$ and $(0, 1)$ are in τ then both the leg and the arm of $(0, 0)$ in τ are positive. Lemma 2.2 then implies that there exist $\mu > \lambda > 0$ such that if the line $x/r + y/s = 1$ cuts off τ then $\mu > r/s > \lambda$. Also, if $(a-1, b-1)$ is an addable cell, then the hyperbolic wall $(r-a)(s-b) = ab$ is an upper boundary of the corresponding region. But then, the region has to lay inside the curved triangle bounded by the lines $r = \mu s$ and $r = \lambda s$, and the hyperbola $(r-a)(s-b) = ab$. □

Lemma 4.7. *Any bounded region is either a triangle or a quadrilateral. Each quadrilateral region has two lower boundaries and two upper boundaries, and they cannot alternate, i.e. the two lower boundaries intersect in a vertex of the region, and the two upper boundaries intersect in a vertex of the region.*

Proof. A bounded region cannot have just two boundaries, since two hyperbolic walls cannot intersect at more than one point (that would correspond to two distinct lines passing through the same two points). In view of Lemma 4.5, the only thing left to check is that a quadrilateral region cannot have sides alternating between lower and upper boundaries.

Let us follow the boundary of a region in the counterclockwise direction, and suppose that at a certain vertex we have a change in the type of the boundary (from lower to upper, or vice versa). Let $(r-a)(s-b)=ab$ be the hyperbola that we followed approaching the vertex, and let $(r-c)(s-d)=cd$ be the hyperbola we followed after the vertex. Perforce, we have $c>a$. Indeed, when moving counterclockwise along a lower boundary, r is decreasing and s is increasing, hence the corresponding line is rotating counterclockwise around (a,b). For the next boundary to be upper, one has to hit the north-east corner (c,d) of an addable cell $(c-1,d-1)$, which has to lie to the east of (a,b) since the line is rotating counterclockwise. The case when the boundary changes from upper to lower is similarly dealt with. One concludes that the upper and lower boundaries cannot always alternate as one moves around the region. □

Lemma 4.8. *Let α be a triangular partition corresponding to a quadrilateral region, which is to say that it has two removable and two addable cells. Then the line touching the two removable cells is parallel to the line touching the two addable cells*[**].

As illustrated in Figure 10, if one moves counterclockwise along the boundary of the (3 sided) region corresponding to $\tau=221$, then the corresponding line successively rotates

- counterclockwise around the north-east corner of the removable cell $(1,1)$ (left),
- clockwise around the north-east corner of the addable cell $(2,0)$ (center),
- and clockwise around the addable cell $(0,3)$ (right).

In a transition from a lower boundary to an upper boundary (left) or vice versa (right), the center of rotation moves east. If the next piece of the boundary is of the same type (center), then the center of rotation moves west.

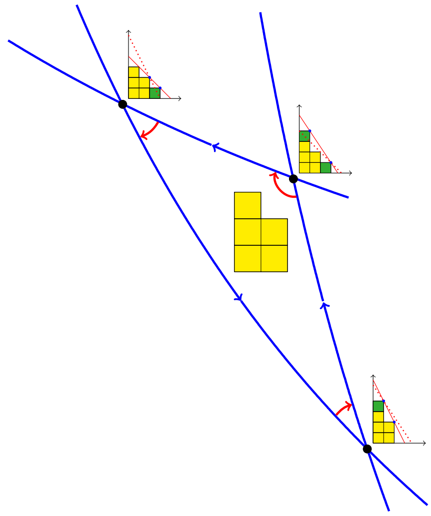

Figure 10: Illustration for Lemma 4.7.

Proof. Let ℓ_1 be the line touching the two removable cells of α, and let ℓ_2 be the line touching the two addable cells of α. Lemma 4.7 implies that $\ell_1,\ell_2\in\overline{R_\alpha}$. Let

$$(i_1,j_1),(i_2,j_2),\ldots,(i_k,j_k),\qquad \text{with}\qquad i_1<i_2<\ldots<i_k,$$

be all the cells touched by ℓ_1, and let

$$(k_1,l_1),(k_2,l_2),\ldots,(k_n,l_n),\qquad \text{with}\qquad k_1<k_2<\ldots<k_n,$$

be all the cells touched by ℓ_2. Since $\ell_1,\ell_2\in\overline{R_\alpha}$, according to Lemma 3.3 the cells $(i_1,j_1),(i_2,j_2),\ldots,(i_k,j_k)$ are in α, and (i_1,j_1) and (i_k,j_k) are the two removable cells of α. Similarly, cells $(k_1,l_1),(k_2,l_2),\ldots,(k_n,l_n)$ are not in α, and (k_1,l_1) and (k_n,l_n) are the two addable cells of α.

Suppose that ℓ_1 and ℓ_2 are not parallel.Let (u,v) be their intersection (here (u,v) is not necessarily in the positive quadrant). Note that all the removable cells should fit below ℓ_2 and none of the addable cells can fit below ℓ_1. It follows that (u,v) is either to the east of the northeast corners of all addable and removable cells, or it is to the west of all of them. Without loss of generality one can assume that (u,v) is to the east,*i.e.* $u<a_1+1$ and $u<c_1+1$.It follows then that the line ℓ_1 is steeper than ℓ_2.

If there is a cell such that its north-east corner is strictly inside the triangle bounded by the horizontal axis and the lines ℓ_1 and ℓ_2, then one gets a contradiction: this cell is strictly below ℓ_2, but cannot be inside α since its north-east corner is above ℓ_1.

One needs to consider two cases. Suppose first that $l_1\geq j_1$. Then there is a cell $(k_1+(i_2-i_1),l_1+(j_2-j_1))$ and its north-east corner is inside the required triangle. Indeed, one has:

$$l_1+(j_2-j_1)\geq j_1+j_2-j_1=j_2\geq 0,$$

[**]In Figure 5 this is reflected by the fact that lines connecting the top and the bottom corners of quadrilateral regions have slopes 1 (in logarithmic scale).

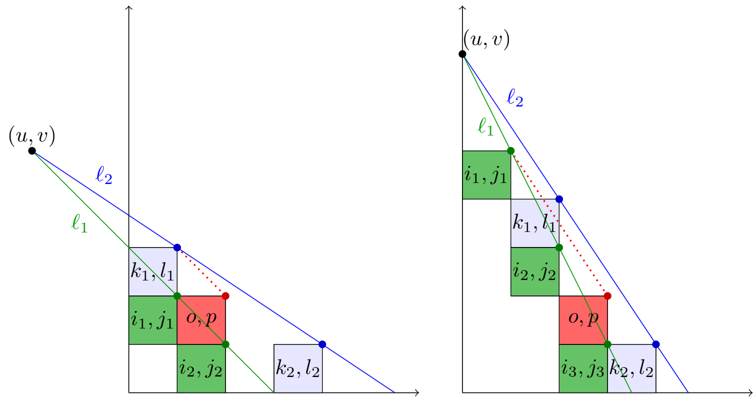

Figure 11: Illustration for Lemma 4.8

and $k_1+(i_2-i_1)>0$, so it is a cell, and its north-east corner is below ℓ_2 and above ℓ_1, because we moved from the cell (k_1, l_1) with the north-east corner on ℓ_2 and above ℓ_1 in the direction parallel to ℓ_1, which goes down steeper than ℓ_2.

Suppose now that $l_1 < j_1$.Then there is a cell $(i_1+(k_2-k_1), j_1+(l_2-l_1))$, and it is inside the required triangle. Indeed, one has:

$$j_1+(l_2-l_1) > l_1+l_2-l_1 = l_2 \geq 0,$$

and $i_1+(k_2-k_1)>0$, so it is a cell, and its north-east corner is below ℓ_2 and above ℓ_1 because we moved from the cell (i_1, j_1) with the north-east corner on ℓ_1 and below ℓ_2 in the direction parallel to ℓ_2, which goes down but less steep than ℓ_1. □

Illustrated in Figure 11, are the cases when $l_1 > j_1$ (left) and $l_1 < j_1$ (right). Correspondingly, on the left $(o,p) = (k_1+(i_2-i_1), l_1+(j_2-j_1))$ and on the right $(o,p) = (i_1+(k_2-k_1), j_1+(l_2-l_1))$. In both instances the cell (o,p) creates a contradiction as it fits under ℓ_2 but not under ℓ_1.

Lemma 4.9. *Suppose that a triangular partition α has two removable cells and just one addable cell (in other words it corresponds to a triangular region with two lower boundaries). Then the line touching the two removable cells does not contain any other positive integer points. Equivalently, no other hyperbolic wall passes through the vertex of the region where the two lower boundaries intersect.*

Proof. Suppose that two parallel lines ℓ_1 and ℓ_2 are such that

1. they both contain integer points,
2. there are no integer points (even not necessarily positive) between them,
3. ℓ_1 contains finitely many positive integer points.

Then ℓ_2 also contains finitely many positive integer points, and the numbers of positive integer points on ℓ_1 and on ℓ_2 differ not more than by one.

Now, let ℓ_1 be the line touching the two removable cells of α, and let ℓ_2 be the line parallel to ℓ_1, above it, and satisfying the above conditions. Clearly, $\ell_2 \in \overline{R_\alpha}$.The statement above then implies that ℓ_2 contains at least one positive integer point. But if it contains more than one positive integer point, then by Lemma 3.3, the eastmost and the westmost cells touched by ℓ_2 are both addable. Contradiction. Therefore, ℓ_2 contains exactly one positive integer point. But then ℓ_1 cannot contain more than two. □

Lemma 4.10. *Suppose that a triangular partition α has just one removable cell and two addable cells (in other words it corresponds to a triangular region with two upper boundaries). Then the line touching the two addable cells does not contain any other positive integer points. Equivalently, no other hyperbolic wall passes through the vertex of the region where the two upper boundaries intersect).*

Proof. Similar to Lemma 4.9. □

The **diagonal** of triangular partition τ, is the set of cells that lie on the segment joining its removable cells. If there is just one such cell, the diagonal is reduced to a single cell. The diagonal acts as a natural "boundary" of τ, and we denote it by ∂_τ. As illustrated in Figure 12, the cells of ∂_τ are corners (either in red or green) of τ. It follows from Lemma 3.3 that the partition $\tau^\circ := \tau \setminus \partial_\tau$, which we call the **interior** of τ, is a triangular

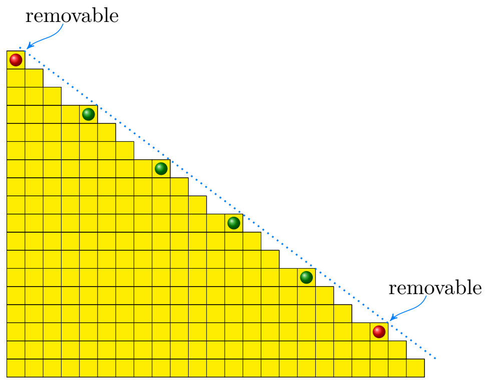

Figure 12: The diagonal of τ is the segment bounded by its removable cells.

partition. Thus, when δ_τ contains k cells, the Hasse diagram of the interval $[\tau^\circ, \tau]$ is a $2k$-sided polygon. In particular, the interval $[\tau_{k-1,k-1}, \tau_{kk}]$ is always $2k$-gon. This is why the whole poset is a mosaic of $2k$-gons, as illustrated in Figure 8.

For a given slope vector $v = (t, 1-t)$, the **ray** R_v is the set of triangular partitions having v as an **admissible** slope vector, *i.e.*

$$R_v := \{\tau \in \mathbb{Y}_\triangle \mid t_\tau^- < t < t_\tau^+\}. \tag{4}$$

This is an infinite chain in $\mathbb{Y}_\triangle$ (see Figure 8). For instance, we have the ray

$$R_{(1-\epsilon,1+\epsilon)} = \{\varepsilon, 1, 2, 21, 31, 32, 321, 421, 431, 432, 4321, \ldots\}.$$

See also an illustration in Figure 8. As any line of irrational slope contains at most one integral point, it follows that for all $n \in \mathbb{N}$ there is one and only one triangular partition of size n on any ray associated with an irrational slope.

5. Triangular Dyck paths

For a given triangular partition τ, we consider the set $\mathcal{D}_\tau := \{\alpha \mid \alpha \subseteq \tau\}$ of **τ-Dyck paths**. Observe that conjugation gives a bijection between $\mathcal{D}_\tau$ and $\mathcal{D}_{\tau'}$. We further write $\mathcal{D}_{(r,s)}$, when $\tau = \tau_{rs}$, and say that its elements are **$(r \times s)$-Dyck paths**. Observe that $\mathcal{D}_{(r,n)} = \mathcal{D}_{(kn,n)}$, for all $kn \leq r \leq kn+1$ and $k \in \mathbb{N}$, since the corresponding triangular partitions coincide. It is often convenient to consider that partitions $\mathcal{D}_\tau$ are padded with zero parts to make them of length $n = l(\tau)+1$. As we have already mentioned, classical Dyck paths correspond to the case $\tau = \tau_{n,n}$, with $n \in \mathbb{N}$. As is very well known, these are counted by the Catalan numbers $\mathcal{A}_n = \frac{1}{n+1}\binom{2n}{n}$. In general, we set $\mathcal{A}_\tau := \#\mathcal{D}_\tau$. For integral partitions τ_{mn}, the greatest common divisor $d = \gcd(m, n)$ plays an interesting role in our story. We have $m = ad$ and $n = bd$, for coprime integers a and b. The cells of τ_{mn} lying on its diagonal $\partial(\tau_{mn})$ are of the form (ak, bk), with $0 < k < d$.

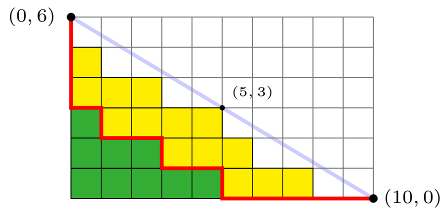

Figure 13: The $\tau_{(10,6)}$-Dyck path 531000.

In preparation for upcoming notions, it will be interesting to consider the skew partition $(\alpha + 1^n)/\alpha$, in which $\alpha + 1^n$ stands for the partition obtained by adding one to each of the parts of α including its zero parts. The above skew partition is readily seen to consist of "independent" columns, as illustrated in Figure 14 with $\alpha = 53100$. The sequence of sizes of these columns is precisely $\mu(\alpha) = 21011$. The choice of n will depend on the context, and it will be larger than the number of parts of α. For a fixed $\tau = \tau_1\tau_2 \cdots \tau_n$, the **$\tau$-area** (or simply **area**) of a τ-Dyck path α is the number of cells lying in the skew shape τ/α. In terms of the **τ-area sequence** $(a_i)_{1\leq i\leq n}$ of α, in which $a_i := \tau_i - \alpha_i$, we clearly have $\mathrm{area}_\tau(\alpha) := \sum_{i=1}^n a_i$.

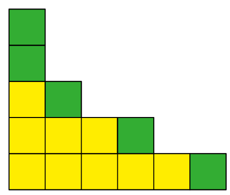

Figure 14: $(\alpha + 1^5)/\alpha$.

Definition 5.1. *For any J subset of $\{i \mid 1 \leq i \leq n\}$, we consider the J-area:*

$$\mathrm{area}_\tau^J(\alpha) := \sum_{i \in J} a_i.$$

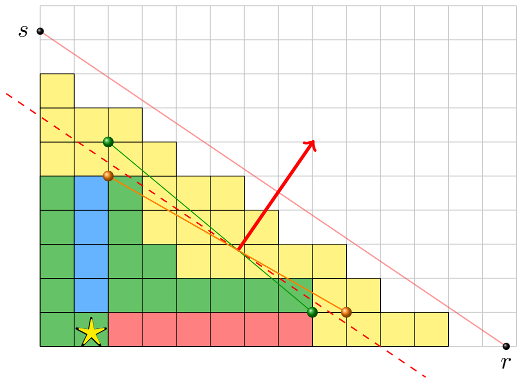

Figure 15: A sim cell of $\alpha = (8, 8, 4, 3, 3)$ relative to $\tau = (12, 10, 9, 7, 6, 4, 3, 1)$.

5.1 Similar cells (Diagonal inversions)

Let τ be a given triangular partition. With the notations of Equation 2, for any $\alpha \subseteq \tau$ consider the set of cells c of α that have hooks in α that are "similar" to τ:

$$\mathrm{Sim}_\tau(\alpha) := \{c \in \alpha \mid t'(c, \alpha) \le t_\tau < t''(c, \alpha))\},$$

where $t_\tau := (t_\tau^- + t_\tau^+)/2$. The cardinality of this set, denoted by $\mathrm{sim}_\tau(\mu)$, is the **similarity index**[††] of μ with respect to τ. Expressed in words, the **similarity index** of μ with respect to τ counts the number of cells of μ having "hook triangle slope vectors" compatible with the (average) slope vector of τ (represented by $\overline{v}$ in Figure 3). Since at corner cells, we have $\ell = 0$ and $a = 0$, we get $\ell/(a + \ell + 1) = 0$ and $(\ell + 1)/(a + \ell + 1) = 1$. Hence, any corner cell of α is always a τ-sim-cells, irrespective of τ. The sim-cells of the partitions contained in $\tau = 32$ are marked by stars in Figure 16.

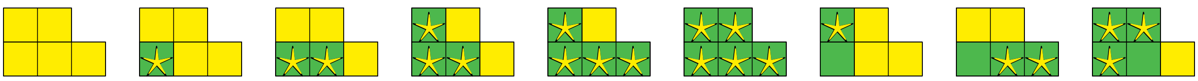

Figure 16: Sim-cells for subpartitions of 32. The first 6 subpartitions are similar to 32.

The following is an example of a sequence of similar triangular partitions:

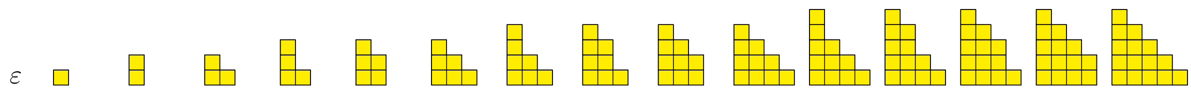

They all share the common slope vector $(1/2 + \epsilon, 1/2 - \epsilon)$.

Lemma 5.1 (with B. Dequêne)**.** *If τ is a triangular partition, then the subpartitions $\alpha \subseteq \tau$ such that $\mathrm{area}_\tau(\alpha) + \mathrm{sim}_\tau(\alpha) = |\tau|$ are exactly those that lie on the ray corresponding to the slope vector $(t_\tau + \epsilon, 1 - t_\tau - \epsilon)$.*

6. Counting τ-Dyck paths

The enumeration of triangular Dyck paths has an interesting (ongoing) history, which has up to now been restricted to the integral case. Even if the simple counting in the case of any integer pairs (m, n) had already been worked out in the 1950s (see [8]), it is only rather recently that the overall enumerative combinatorics community has become aware of that fact. For a long time, only the "coprime case" was deemed really understood, recently going under the name of rational Catalan combinatorics. These include the classical **Fuss-Catalan** numbers when $m = kn$ (or equivalently when $m = kn+1$). A direct extension of the classical "cycling" argument shows that, for m and n coprime integers, the number (m, n)-Dyck paths is given by the formula

$$\mathcal{A}_{mn} = \frac{1}{m+n}\binom{m+n}{n}. \tag{5}$$

A formula for the non-coprime case of τ_{mn} is described in the next subsection.

[††]This just another name for the "dinv" statistic, that we choose to stress its natural geometrical meaning.

6.1 Bizley formula

In the general "integral" situation, the enumeration formula of $(m \times n)$-Dyck paths takes the form of a sum of terms indexed by partitions of the greatest common divisor of m and n. This is what makes it harder to "guess" a formula[‡‡], since the numbers obtained do not factor nicely in general, even if they are effectively sums of nicely factorized numbers. The **Grossman-Bizley** formula (see [8]) is:

$$\mathcal{A}_{mn} := \sum_{\alpha \vdash d} \frac{1}{z_\alpha} \prod_{k \ \text{part of}\ \alpha} \frac{1}{a+b} \binom{k(a+b)}{ka}, \tag{6}$$

where $(m,n) = (ad, bd)$ with a and b coprime, so that $d = \gcd(m,n)$. It is worth recalling that $d!/z_\alpha$ is the number of sizes d permutations of cycle type α, with

$$z_\alpha := \prod_i i^{c_i}\, c_i!,$$

where α has c_i parts of size i. Specific examples of Equation 6 are:

$$\begin{aligned} \mathcal{A}_{2a,2b} &= \tfrac{1}{2}\left(\tfrac{1}{a+b}\tbinom{a+b}{a}\right)^2 + \tfrac{1}{2}\left(\tfrac{1}{a+b}\tbinom{2a+2b}{2a}\right), \\ \mathcal{A}_{3a,3b} &= \tfrac{1}{6}\left(\tfrac{1}{a+b}\tbinom{a+b}{a}\right)^3 + \tfrac{1}{2}\left(\tfrac{1}{a+b}\tbinom{a+b}{a}\right)\left(\tfrac{1}{a+b}\tbinom{2a+2b}{2a}\right) + \tfrac{1}{3}\left(\tfrac{1}{a+b}\tbinom{3a+3b}{3a}\right). \end{aligned} \tag{7}$$

Observe that, for fixed coprime numbers a and b, all the formulas for $(m,n) = (ad, bd)$, with $0 \le d$, may be presented in the form of the generating function:

$$\sum_{d=1}^{\infty} \mathcal{A}_{ad,bd}\ z^d = \exp\Big(\sum_{k\ge 1} \tfrac{1}{a+b}\tbinom{k(a+b)}{ka}\, z^k/k\Big). \tag{8}$$

As it happens, this is a specialization of more general formula (see Equation 33).

6.2 Explicit number of Dyck paths for all triangular partitions

For all triangular partitions, τ of size at most 9, the number $\mathcal{A}_\tau$ of τ-Dyck paths may be found in the Table 1. In the next subsection, we will see how to calculate these numbers recursively.

1											
2											
1^2	2										
3	3										
1^3	21	3									
4	5	4									
1^4	21^2	31	4								
5	7	7	5								
1^5	21^3	2^21	32	41	5						
6	9	9	9	9	6						
1^6	21^4	2^21^2	321	42	51	6					
7	11	12	14	12	11	7					
1^7	21^5	2^21^3	3211	421	52	61	7				
8	13	15	19	19	15	13	8				
1^8	21^6	2^21^4	2^31^2	32^21	431	53	62	71	8		
9	15	18	18	23	23	18	18	15	9		
1^9	21^7	2^21^5	2^31^3	32^21^2	3^221	432	531	63	72	81	9
10	17	21	2^2	30	28	28	30	2^2	21	17	10

Table 1: Number of τ-Dyck paths

6.3 General recursive formula for triangular partitions

For any partition triangular τ, the q-area enumerator of τ-Dyck paths is

$$\mathcal{A}_\tau(q) := \sum_{\alpha \subseteq \tau} q^{\mathrm{area}_\tau(\alpha)}. \tag{9}$$

Since conjugation is an area-preserving bijection between the set of τ-Dyck paths and the set of τ'-Dyck paths, we clearly have $\mathcal{A}_\tau(q) = \mathcal{A}_{\tau'}(q)$. In preparation for the upcoming proposition, let us consider the following

[‡‡]Most guessing approaches rely (directly or indirectly) on the fact the numbers considered have nice factorization in small prime numbers.

notions. The **bounding word** w_μ, of a partition μ, encodes the simplest southeast lattice path such that the cells of the diagram of μ are those that sit below w_μ. Thus $w_\mu := 0^{r_k}1\cdots 0^{r_2}1\cdots 0^{r_1}1$, where $r_k = \mu_k$, and $r_i = \mu_i - \mu_{i+1}$, for $1 \le i < k$. For two partitions α and β, we denote by $\alpha \odot \beta$ the partition whose bounding word/path is the concatenation of words: $w_\alpha \cdot w_\beta$. The empty partition acts as the identity for this associative product. Three-way decompositions of the form $\nu = \alpha \odot \gamma \odot \beta$, with γ indicating a one cell partition, will be of special interest. Observe that the middle one cell partition "γ" necessarily corresponds to a corner of ν. For example, Let us denote by $\Delta(\tau)$ the set of pairs (α, β) corresponding to three-way decompositions of τ, of the

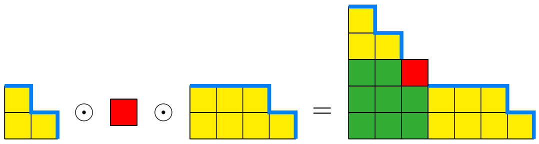

Figure 17: A decomposition $\alpha \odot \gamma \odot \beta$.

form $\tau = \alpha \odot \gamma \odot \beta$, with the corner cell γ sitting on the diagonal of τ. In formula,

$$\Delta(\tau) := \{(\alpha, \beta) \mid \tau = \alpha \odot \gamma \odot \beta, \quad \text{and} \quad \gamma \in \partial_\tau\}. \tag{10}$$

Recall also that τ° stands for the interior of τ, which is obtained by removing from τ all the cells on its diagonal. Then, the number $\mathcal{A}_\tau$ of τ-Dyck paths may efficiently be calculated with the following recursive formula.

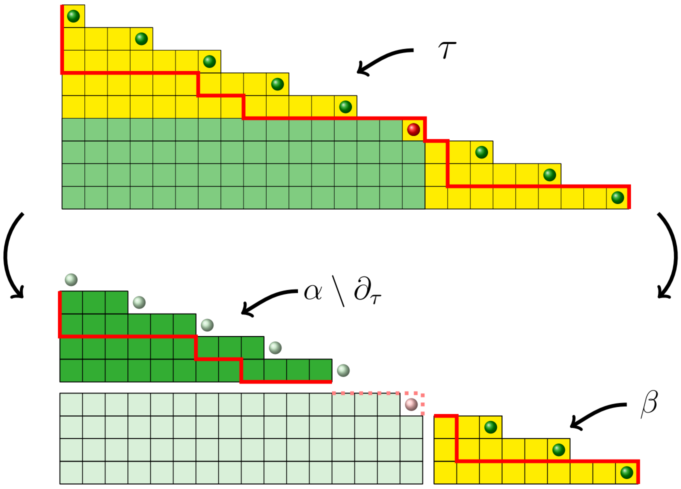

Figure 18: First return cell ●, with ● marking other diagonal cells.

Proposition 6.1. *Denoting by $\partial = \partial_\tau$ the diagonal of a given triangular partition τ, then for the q-area enumerator of τ-Dyck, we have the recurrence*

$$\mathcal{A}_\tau(q) = q^{|\partial|}\,\mathcal{A}_{\tau^\circ}(q) + \sum_{(\alpha,\beta)\in\Delta(\tau)} q^{|\alpha\cap\partial|}\,\mathcal{A}_{\alpha\setminus\partial}(q)\,\mathcal{A}_\beta(q), \tag{11}$$

with initial condition $\mathcal{A}_\varepsilon(q) = 1$. In particular, setting $q = 1$, we have

$$\mathcal{A}_\tau = \mathcal{A}_{\tau^\circ} + \sum_{(\alpha,\beta)\in\Delta(\tau)} \mathcal{A}_{\alpha\setminus\partial}\,\mathcal{A}_\beta. \tag{12}$$

This is a direct generalization of the well-known classical recurrence for Dyck path. Its proof corresponds to a suitably adapted "first return to diagonal" argument typically used in the proof of the classical case (see Figure 18). It is noteworthy that all possible $\alpha \setminus \partial$ and β that occur in the right-hand side of Equation 11 are triangular, as they are respectfully factors of τ° and τ. Hence, for a given partition τ, the set of partitions that will arise in the recurrence can only be factors (for the $\odot$-product) of partitions obtained by successive removal of diagonals. Hence, they all have a slope in common with that of τ.

The q-area enumerators for all triangular partitions of size at most 6 are as follows (avoiding repetitions for conjugate partitions):

$$
\begin{array}{llll}
\mathcal{A}_1 = & q+1, & \mathcal{A}_2 = & q^2+q+1, \\
\mathcal{A}_{21} = & q^3+q^2+2q+1, & \mathcal{A}_3 = & q^3+q^2+q+1, \\
\mathcal{A}_{31} = & q^4+q^3+2q^2+2q+1, & \mathcal{A}_4 = & q^4+q^3+q^2+q+1, \\
\mathcal{A}_{32} = & q^5+q^4+2q^3+2q^2+2q+1, & \mathcal{A}_{41} = & q^5+q^4+2q^3+2q^2+2q+1, \\
\mathcal{A}_5 = & q^5+q^4+q^3+q^2+q+1, & \mathcal{A}_{321} = & q^6+q^5+2q^4+3q^3+3q^2+3q+1, \\
\mathcal{A}_{42} = & q^6+q^5+2q^4+2q^3+3q^2+2q+1, & \mathcal{A}_{51} = & q^6+q^5+2q^4+2q^3+2q^2+2q+1, \\
\mathcal{A}_6 = & q^6+q^5+q^4+q^3+q^2+q+1. & &
\end{array}
$$

6.4 Counting by Area and Sim

As in [9], we may consider the enumeration of τ-Dyck paths with respect to two statistics: "area" and "sim", in the triangular case. Note that our "sim" is the "dinv" of *loc. cit.*. The resulting (q,t)-polynomials:

$$\mathcal{A}_\tau(q,t) := \sum_{\alpha\subseteq\tau} q^{\mathrm{area}_\tau(\alpha)} t^{\mathrm{sim}_\tau(\alpha)}, \tag{13}$$

plays a central role in a wide range of subjects. Once again, applying conjugation to partitions α contained in τ, it is easy to check that $\mathcal{A}_{\tau'}(q,t) = \mathcal{A}_\tau(q,t)$. It follows from Lemma 5.1 that, for any triangular partition τ of size n, we have

$$\begin{aligned}\mathcal{A}_\tau(q,t) &= (q^n + q^{n-1}t + \ldots + qt^{n-1} + t^n) + \ldots, \\ &= s_n(q,t) + \ldots\end{aligned} \tag{14}$$

where the remaining terms are of degree (strictly) less than n. In the particular case $\delta_k = (k, k-1, \ldots, 2, 1, 0)$, one may further see that

$$\mathcal{A}_{\delta_k}(q,t) = s_{\binom{k+1}{2}}(q,t) + \Big(\sum_{j=\binom{k}{2}}^{\binom{k+1}{2}-2} s_{j,1}(q,t)\Big) + \ldots, \tag{15}$$

with the missing terms only involving Schur functions indexed by partitions having a second part larger or equal to 2. Taking into account the symmetry $\mathcal{A}_\tau = \mathcal{A}_{\tau'}$ to avoid unnecessary repetitions, the values of $\mathcal{A}_\tau$ for (all) triangular partitions of size at most 8 are as given in Table 2. The entries are expressed in terms of Schur functions $s_\mu = s_\mu(q,t)$, so that the Schur positivity (see next section) is made apparent.

$(0, \mathbf{1})$				
$(1, s_1)$				
$(2, s_2)$				
$(21, s_{11}+s_3)$	$(3, s_3)$			
$(31, s_{21}+s_4)$	$(4, s_4)$			
$(32, s_{31}+s_5)$	$(41, s_{31}+s_5)$	$(5, s_5)$		
$(321, s_{31}+s_{41}+s_6)$	$(42, s_{22}+s_{41}+s_6)$	$(51, s_{41}+s_6)$	$(6, s_6)$	
$(421, s_{32}+s_{41}+s_{51}+s_7)$	$(52, s_{32}+s_{51}+s_7)$	$(61, s_{51}+s_7)$	$(7, s_7)$	
$(431, s_{42}+s_{51}+s_{61}+s_8)$	$(53, s_{42}+s_{61}+s_8)$	$(62, s_{42}+s_{61}+s_8)$	$(71, s_{61}+s_8)$	$(8, s_8)$

Table 2: Table of values $(\tau, \mathcal{A}_\tau)$.

A constant term formula for $\mathcal{A}_\tau(q,t)$ is given in [9, Prop. 7.2.1]. It follows that $\mathcal{A}_\tau(q,t)$ is symmetric in q and t, even though this is not evident in Equation 13. Setting $t = 1/q$, we often get nice product formulas. For instance, In the case of τ_{ab}, with a and b coprime integers, we have

$$q^{|\tau_{ab}|}\mathcal{A}_{\tau_{ab}}(q,1/q) = \frac{1}{[a+b]_q}\begin{bmatrix}a+b\\ a\end{bmatrix}. \tag{16}$$

For any triangular partition $\tau = (k,j)$, with two parts, we further have

$$q^{|\tau|}\mathcal{A}_\tau(q,1/q) = \frac{[2k-j+2]_q[3(j+1)]_q}{[3]_q[2]_q}. \tag{17}$$

7. Generic Schur function expansion

The polynomials $\mathcal{A}_\tau(q,t)$ are not only symmetric but extensive explicit calculations suggest that they always expand positively on the Schur polynomials basis. The following conjecture of [9, Conj. 7.1.1] is supported by extensive calculations (for all triangular partitions of $n \leq 28$); and in some instances proofs and/or justifications via representation theory (see [6, 12]).

Conjecture 7.1. *For any triangular partition τ of size n, the polynomial $\mathcal{A}_\tau(q,t)$ affords a positive Schur-expansion*

$$\mathcal{A}_\tau(q,t) := \sum_\lambda c_\lambda^\tau\, s_\lambda(q,t), \qquad i.e. \text{ with coefficients} \qquad c_\lambda^\tau \in \mathbb{N}. \tag{18}$$

The sum runs over (length ≤ 2) partitions λ such that $|\lambda| \leq |\tau|$.

Specific values are:

$$\mathcal{A}_{(n-k,k)} = \sum_{j=0}^{k} s_{(n-2j,j)}, \tag{19}$$

whenever $n > 3k-1$, and $\mathcal{A}_{2k-1,k} = \mathcal{A}_{2k,k-1}$. This exhaust all possibilities for two-part triangular partitions, since we must have $n \geq 3k-1$ if we want $\tau = (n-k,k)$ to be triangular. See [11, section 3]

7.1 Several parameters

Conjecturally, there is a natural extension of the previous Schur-expansions that encompass situations involving more parameters, hence involving Schur functions indexed by partitions having more than two parts. In some instances these are obtained as the GL_k-character of the $\mathbb{S}_n$-alternating component of representations of $GL_k \times \mathbb{S}_n$, as discussed in [5–7], thus explaining the Schur positivity. In the representation theoretical framework, one can show that these expressions become stable once $k \geq n$. We may thus present them as positive integer coefficient linear combination of "formal" Schur expansions $s_\lambda(\boldsymbol{q}) = s_\lambda(q_1, q_2, \ldots, q_k)$:

$$\mathcal{A}_\tau(\boldsymbol{q}) := \sum_{|\lambda| \leq |\tau|} c_\lambda^\tau\, s_\lambda(\boldsymbol{q}). \tag{20}$$

Writing $\rho(\tau)$ for $\min(l(\tau), l(\tau'))$, we may summarize our theoretical and experimental observations about these as follows:

1. for all τ:
$$\mathcal{A}_\tau(q,t) = \sum_{\alpha \subseteq \tau} t^{\mathrm{sim}_\tau(\alpha)} q^{\mathrm{area}_\tau(\alpha))}; \tag{21}$$

2. for all τ,
$$\mathcal{A}_\tau(\boldsymbol{q}) = \mathcal{A}_{\tau'}(\boldsymbol{q}); \tag{22}$$

3. if λ has more than $\rho(\tau)$ parts, then $c_\lambda^\tau = 0$;

4. if $c_\lambda^\tau \neq 0$, then $|\lambda| + \binom{l(\lambda)}{2} \leq |\tau|$;

5. if $\tau = \tau' + \tau_{n,n}$, with τ' triangular of length at most n, then
$$e_n^\perp \mathcal{A}_\tau(\boldsymbol{q}) := \mathcal{A}_{\tau'}(\boldsymbol{q}), \tag{23}$$

6. for any τ,
$$(e_k^\perp \mathcal{A}_\tau)(q) = q^{|\tau| - \binom{k+1}{2}} \begin{bmatrix} \rho(\tau) \\ k \end{bmatrix}_{1/q}. \tag{24}$$

7. for all k and n such that $0 \leq k \leq n-1$, and $\tau := \tau_{n,n}$, then
$$(e_{n-k-1}^\perp \mathcal{A}_\tau)(q,t) := \sum_{\alpha \subseteq \tau} t^{\mathrm{sim}_\tau(\alpha)} \Big(\sum_{\substack{\mathrm{des}(\alpha) \subseteq J \\ |J| = k}} q^{\mathrm{area}_\tau^J(\alpha)} \Big), \tag{25}$$

where the second summation runs over subsets J of $\{i \,|\, 1 \le i \le n-1\}$ that satisfy the stated requirements. To finish parsing the right-hand side of this last equality, we recall Definition 5.1, and set

$$\mathrm{des}(\alpha) := \{i \,|\, 1 \le i \le n-1, \text{ and } \alpha_i > \alpha_{i+1}\}. \tag{26}$$

We underline that this right-hand side is exactly the combinatorial description of the coefficient of e_n in the Delta theorem. Extending this equality to any triangular partition would thus have an interesting impact on possible extensions of this theorem.

Besides cases already covered, some experimentally calculated values are as follows

$$\begin{aligned}
\mathcal{A}_{321} &= s_{111} + s_{31} + s_{41} + s_{6},\\
\mathcal{A}_{421} &= s_{211} + s_{32} + s_{41} + s_{51} + s_{7},\\
\mathcal{A}_{431} &= s_{311} + s_{42} + s_{51} + s_{61} + s_{8},\\
\mathcal{A}_{432} &= s_{411} + s_{33} + s_{52} + s_{61} + s_{71} + s_{9},\\
\mathcal{A}_{531} &= s_{221} + s_{411} + s_{42} + s_{52} + s_{61} + s_{71} + s_{9},\\
\mathcal{A}_{532} &= s_{311} + s_{521} + s_{43} + s_{52} + s_{62} + s_{71} + s_{81} + s_{10.},\\
\mathcal{A}_{631} &= s_{311} + s_{521} + s_{43} + s_{52} + s_{62} + s_{71} + s_{81} + s_{10.},\\
\mathcal{A}_{4321} &= s_{1111} + s_{311} + s_{411} + s_{511} + s_{42} + s_{43} + s_{61} + s_{62} + s_{71} + s_{81} + s_{10.},\\
\mathcal{A}_{54321} &= s_{11111} + s_{3111} + s_{4111} + s_{5111} + s_{6111} + s_{611} + s_{711} + 2\,s_{811} + s_{911} + s_{10.11} + s_{421} + s_{521}\\
&\quad + s_{621} + s_{721} + s_{821} + s_{431} + s_{531} + s_{631} + s_{441} + s_{44} + s_{64} + s_{74} + s_{63} + s_{73} + s_{83}\\
&\quad + s_{93} + s_{72} + s_{82} + s_{92} + s_{10.2} + s_{10.1} + s_{11.1} + s_{11.2} + s_{12.1} + s_{13.1} + s_{15.}.
\end{aligned}$$

Observe that one may “predict” the equality $\mathcal{A}_{532} = \mathcal{A}_{631}$ using Equation 22 in conjunction with Equation 23, since $532 = 211 + 321$, $631 = 31 + 321$, and 31 is the conjugate of 211. Observe in $\mathcal{A}_{54321}$ that some coefficients are larger than 1. Although these last values may be simply inferred just from the knowledge of Equation 25, they do agree with representation theoretical descriptions not discussed here. For more on this see [4].

7.2 Hook shape component

A classical plethystic evaluation of Schur functions makes it easy to restrict a symmetric function to its “hook shape component”. Indeed, recall that

$$\frac{1}{u+v} s_\mu[u - \varepsilon v] := \begin{cases} u^a v^b & \text{if } \mu = (a \,|\, b),\\ 0 & \text{otherwise,}\end{cases} \tag{27}$$

using Frobenius notation for hooks, and with ε standing for a “formal plethystic variable” such that $f[\varepsilon \boldsymbol{x}] = \omega f(\boldsymbol{x})$. Then, it is easy to show that

Proposition 7.1. *Assuming Equation 24,*

$$\frac{1}{u+v}\mathcal{A}_\tau[u - \varepsilon v] = \sum_{a+b=n-1} c^\tau_{(a\,|\,b)} u^a v^b = u^{|\tau|} \prod_{i=1}^{\rho(\tau)-1} \left(1 + \frac{v}{u^i}\right). \tag{28}$$

where $\rho(\tau) := \min(l(\tau), l(\tau'))$.

In other words, the multiplicity of a hook indexed Schur function $s_{(a\,|\,b)}$ in $\mathcal{A}_\tau$ is the coefficient of $u^a v^b$ in Equation 28. For instance, the above formula gives 16 of the 37 terms of $\mathcal{A}_{54321}$, leaving only 21 terms to be explained:

$$\begin{aligned}
\mathcal{A}_{54321} = (16 \text{ terms}) &+ s_{421} + s_{521} + s_{621} + s_{721} + s_{821} + s_{431} + s_{531} + s_{631} + s_{441}\\
&+ s_{44} + s_{64} + s_{74} + s_{63} + s_{73} + s_{83} + s_{93} + s_{72} + s_{82} + s_{92} + s_{10.2} + s_{11.2}.
\end{aligned}$$

The remaining terms may be obtained using Equation 25.

A striking fact is that $\mathcal{A}_\tau[\boldsymbol{z} - \varepsilon a]$ essentially corresponds to the triply graded Poincaré series of the Khovanov-Rozansky homology of some torus knots, for adequate choices of τ.

8. Triangular parking functions

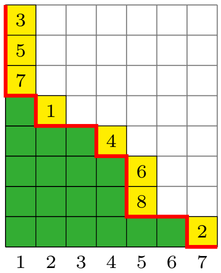

Figure 19: Parking function.

For any partition α and $n \geq l(\alpha)$, a height n **parking function** of form α is simply a standard tableau π of shape $(\alpha+1^n)/\alpha$. Observe that the skew partition $(\alpha+1^n)/\alpha$ is a set of disjoint columns, say of respective size c_i. It follows readily that the number of standard tableaux considered is:

$$\frac{n!}{c_1!c_2!\cdots c_k!}, \tag{29}$$

Observe also that the skew Schur function $s_{(\alpha+1^n)/\alpha}$ is equal to

$$s_{(\alpha+1^n)/\alpha} = e_{c_1} e_{c_2} \cdots e_{c_k}. \tag{30}$$

Given a triangular partition τ and $n \geq l(\tau)$, the overall set τ**-parking functions** of height n, is the set $\{\pi \,|\, \pi \in \text{SYT}((\alpha+1^n)/\alpha), \text{ and } \alpha \subseteq \tau\}$ which we denote by $\mathcal{E}_{(\tau,n)}$. For $\tau = \tau_{mn}$, with (m,n) coprime integers, the total number of τ-parking functions (of height n) is well known to be equal to m^{n-1}. More generally, for $\tau = \tau_{mn}$ with $(m,n) = (da, db)$, such that a, b coprime and $d = \gcd(m,n)$, we also have a parking function analog of Equation 6:

$$\#\mathcal{E}_{(\tau_{mn},n)} = \sum_{\lambda \vdash d} \frac{1}{z_\lambda} \binom{n}{\lambda} \prod_{k\in\lambda} \frac{1}{a}(ka)^{kb-1}. \tag{31}$$

8.1 Symmetric function counting

It is natural to extend the above enumeration to a symmetric function q-enumeration of height n parking functions, setting:

$$\mathcal{E}_{(\tau,n)}(q;\boldsymbol{x}) := \sum_{\alpha\subseteq\tau} q^{|\tau|-|\alpha|}\, s_{(\alpha+1^n)/\alpha}(\boldsymbol{x}). \tag{32}$$

In the special cases $\tau = \tau_{(da,db)}$, with a, b coprime, there is (see [2,3]) a symmetric function version of Equation 8:

$$\sum_{d=1}^{\infty} \mathcal{E}_{(\tau_{(da,db)},db)}(1;\boldsymbol{x})\ z^d = \exp\Big(\sum_{k\geq 1} \tfrac{1}{a} e_{kb}[ka\,\boldsymbol{x}]\, z^k/k\Big). \tag{33}$$

We have the following nice extension of Equation 11 for the symmetric function enumeration of parking functions, whose proof follows a very similar argument.

Proposition 8.1. *For any triangular partition τ and any $n > l(\tau)$, the generic symmetric function enumerator of τ-parking functions satisfies the recurrence*

$$\mathcal{E}_{(\tau,n)}(q;\boldsymbol{x}) = q^{|\delta|}\mathcal{E}_{(\tau^\circ,n)}(q;\boldsymbol{x}) + \sum_{(\alpha,\beta,k)} q^{|\alpha\cap\delta|}\mathcal{E}_{(\alpha\setminus\partial,n-k)}(q;\boldsymbol{x})\,\mathcal{E}_{(\beta,k)}(q;\boldsymbol{x}), \tag{34}$$

with initial condition $\mathcal{E}_{\varepsilon,n}(\boldsymbol{x}) = e_n(\boldsymbol{x})$, and where the summation runs over the set of triples (α,β,k) such that $\tau = \alpha \odot 1 \odot \beta$, with the partition 1 corresponding to a cell (i,k) of the diagonal $\partial = \partial_\tau$ of τ.

Formulas for a q,t-enumeration of τ-parking functions with special values of n may be found in [9]. One may extend these for general values of n, and there are stable several parameter (*i.e.* $\boldsymbol{q} = (q_1, q_2, \ldots, q_k)$) extensions of the form:

$$\mathcal{E}_{\tau,n}(\boldsymbol{q},\boldsymbol{x}) = \sum_{\mu\vdash n}\sum_{\lambda} c_{\lambda\mu} s_\lambda(\boldsymbol{q})\, s_\mu(\boldsymbol{x}),$$

which specialize at $\boldsymbol{q} = (q,t)$ to the above-mentioned (q,t)-enumeration. This is ongoing work.

Acknowledgments

F.B. acknowledges the support of the Natural Sciences and Engineering Research Council of Canada (NSERC). M. M. was partially supported by the Simons Collaboration grant 524324. M. M. is also grateful to MSRI for its hospitality during Winter-Spring 2022.

References

[1] D. Armstrong, N. A. Loehr, and G. S. Warrington, *Rational parking functions and Catalan numbers*, Ann. Combin. 20:1 (2016), 21–58.

[2] D. Armstrong, V. Reiner, and B. Rhoades, *Parking spaces*, Adv. Math. 269 (2015), 647–706.

[3] J.-C. Aval and F. Bergeron, *A note on: rectangular Schröder parking functions combinatorics*, Sém. Lothar. Combin. 79 ([2018–2020]), Article B79a.

[4] F. Bergeron, *Multivariate diagonal coinvariant spaces for complex reflection groups*, Adv. Math. 239 (2013), 97–108.

[5] F. Bergeron, *Open questions for operators related to rectangular Catalan combinatorics*, J. Comb. 8:4 (2017), 673–703.

[6] F. Bergeron, $(GL_k \times S_n)$*-modules and nabla of hook-indexed Schur functions*, 2019, `https://arxiv.org/abs/arXiv:1909.03531`.

[7] F. Bergeron, $(GL_k \times S_n)$*-Modules of Multivariate Diagonal Harmonics*, 2020, `https://arxiv.org/abs/arXiv:2003.07402`.

[8] M. T. L. Bizley, *Derivation of a new formula for the number of minimal lattice paths from* $(0, 0)$ *to* (km, kn) *having just* t *contacts with the line* $my = nx$ *and having no points above this line; and a proof of Grossman's formula for the number of paths which may touch but do not rise above this line*, J. Inst. Actuar. 80 (1954), 55–62.

[9] J. Blasiak, M. Haiman, J. Morse, A. Pun, and G. H. Seelinger, *A Shuffle Theorem for Paths Under Any Line*, 2021, `https://arxiv.org/abs/arXiv:2102.07931`.

[10] S. Corteel, G. Rémond, G. Schaeffer, and H. Thomas, *The number of plane corner cuts*, Adv. in Appl. Math. 23:1 (1999), 49–53.

[11] E. Gorsky, G. Hawkes, A. Schilling, and J. Rainbolt, *Generalized* q, t*-Catalan numbers*, Algebr. Comb. 3:4 (2020), 855–886.

[12] J. Haglund, J. B. Remmel, and A. T. Wilson, *The Delta conjecture*, Trans. Amer. Math. Soc. 370:6 (2018), 4029–4057.

[13] M. Lothaire, *Algebraic combinatorics on words*, Encyclopedia of Mathematics and its Applications, volume 90, Cambridge University Press, Cambridge, 2002.

[14] I. Müller, *Corner cuts and their polytopes*, Beiträge Algebra Geom. 44:2 (2003), 323–333.

[15] S. Onn and B. Sturmfels, *Cutting corners*, Adv. in Appl. Math. 23:1 (1999), 29–48.

[16] C. R. Platt, *Planar lattices and planar graphs*, J. Combinatorial Theory Ser. B 21:1 (1976), 30–39.